Iran University of Science and Technology

Automotive Science and Engineering

Journal Homepage: ase.iust.ac.ir

ISSN: 2008-9899

Forcing Frequency Analysis and Control of Chaos in Vehicle Dynamics Using Time delay feedback Algorithm

Yavar Nourollahi Golouje[1], Seyyed Mahdi Abtahi[1*], Majid Majidi[1]

[1] Department of Mechanical Engineering, Faculty of Industrial and Mechanical Engineering, Qazvin Branch,Islamic Azad University, Qazvin, Iran

ARTICLE INFO

Article history:
Received: 4 October 2022
Accepted: 11 October 2022
Published: 11 October 2022

Keywords:
Forcing frequency
power consumption
Chaos control
Time delay feedback

ABSTRACT

The chaos analysis and chaos control system has been considered for the heave dynamics in this paper. In the first part of this work, dynamical model of the vehicle system is derived using the Newtonian dynamics. After simulation of the model, nonlinear behaviors consist of jump phenomenon and chaos in the heave motion of vehicle are studied using the forcing frequency tool that depicts the root to chaos from the periodic orbits. In the second part of this paper, controller system based on developed delay feedback scheme is designed to stabilize the unstable trajectories. For elimination of chaos phenomenon in the vertical dynamics, a novel sliding delay feedback controller is developed via the fuzzy inference system on the active suspension. In the controller structure, fuzzy logic can tune online the controller gain of the sliding delay feedback system in order to reject the chattering phenomenon in the sliding mode algorithm. Results of the simulations in control system show the enhancements of responses of feedback system with reducing the power consumption of system and eliminating of chaos.

*Corresponding Author
Email Address: m.abtahi@qiau.ac.ir
https://doi.org/10.22068/ase.2022.616

1. Introduction

The first chaos control system called OGY was designed by Ott et al (1990) based on linearization of Poincare' sections to stabilize Unstable Periodic Orbits (UPOs). Implementation of the OGY controller in the chaotic systems requires a complex solution of the system's unstable orbits, and the controller is activated when the system dynamics reach near the fixed point. In 1992, Pyragas introduced the delay feedback control method for controlling the chaotic systems, which controls immediately the system that there is no need to solve the UPOs. Other limitation of the OGY method compared to Pyragas is the derivation of the Poincare' sections, along with high sensitivity of the chaotic system relative to change the parameters in keeping away the periodic orbits from the basin of attraction [1-4]. Recently, many studies have been done on chaotic dynamics as well as chaos control of vehicle vibrations. For example, Litak and his colleagues investigated the chaotic vibrations and chaotic control of vehicle in quadratic model under the sinusoidal unevenness of the road surface [5, 6]. Naik and Singru analyzed the stability, resonance, and chaos in the vehicle's vertical dynamics using the Melnikov standard [7]. Also, the effect of damping factor on dynamic behaviour is investigated by analyzing the bifurcation diagrams in the bounce model along with determining the specific frequency and time lag between wheels in the excitation force of the road surface under chaos [8, 9]. Fakheari et al studied the effect of uneven speed control parameters and the passengers on the vehicle's chaotic vibrations. Also, the chaotic vibrations in a vehicle equipped with magnetic dampers are controlled using a return control method [10, 11]. Delay feedback control system has been used in the vehicle control systems due to its simplicity in design and good performance. Among them, this method is used in the active suspension system to stabilize the rotational oscillations of the vehicle body [12]. Zhang et al controlled the chaotic lateral dynamic of the electric vehicle by active steering system using the adaptive time delay feedback method. Also, the stability of the vehicle was analyzed with delay feedback control, which led to the reduction of vehicle vibrations despite the hop bifurcation in the system [13-15]. In this work, the chaotic oscillations in vertical model of vehicle were controlled using the delay feedback control algorithm developed by the fuzzy sliding mode system. For this purpose, after modelling and simulation of the system without controller, chaos was analysed in nonlinear dynamics through forcing frequency diagrams. Furthermore, the forcing frequency and power consumption was measured in the nonlinear dynamical system with respect to the control parameters of the road excitation and the control variables in the active suspension for designing of chaos controller. In order to better stabilize the Time delay feedback method, a sliding mode algorithm has been integrated in its structure, which has used fuzzy inference to Time delay feedback the sliding delay feedback. In this control strategy, by online calculation of the controller's coefficient in the developed Pyragas control system based on the sliding mode, the appropriate value of the control gain was obtained via the fuzzy system that the chattering phenomenon caused by the sliding mode behaviour around the sliding surface can be eliminated. The simulation results of the feedback system confirmed the stabilization of the active suspension system along with overcoming chaos that occurs in the vehicle.

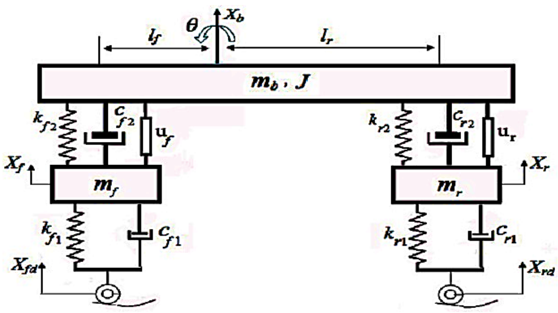

Figure 1: Model of vehicle with active suspension system under the road roughness

2. Vehicle dynamics modeling

The vertical model of open-loop system in vehicles with active suspension is demonstrated in figure 1. The model consists of the main rigid body and two tires. State variables of the system are heave motion (x_b) and rotation of main body (θ). Also, vertical motions of front and rear tires are stated as (x_f) and (x_r).

In this modelling process, rotations around the other axis are neglected. Also, all of springs and dampers in the suspension system and tire model are considered with nonlinear effects and the front and rear actuators force in the active suspension system are modeled as u_f and u_r respectively.

Nonlinear model of springs and dampers in the suspension system are as follows [16]:

$$F_S = K_1X + K_2X^3 = K_1(x_b - x_0) + K_2(x_b - x_0)^3$$
$$F_{SC} = C_1V + C_2V^3 = C_1\frac{d}{dt}(x_b - x_0) + C_2(\frac{d}{dt}(x_b - x_0))^3 \quad (1)$$

where, K and C are the stiffness coefficient of the spring and dampers of the suspension system. X_0 is the displacement of the input excitation from the road surface that is assumed as an alternating sinusoidal function and expressed by $X_{fd} = A\sin(2\pi ft)$ and $X_{rd} = A\sin(2\pi ft + \alpha)$ for the front and rear tires, respectively, where A is the amplitude, *f* is the frequency of the excitation force and α represents the time delay between the displacement applied by the unevenness of the road surface affecting the front and rear tires. Also, vehicle tires are modeled with non-linear spring and viscous damper, and the mathematical relationship for tire spring force equals $f_s = k_s(\zeta_s)$ and $f_{tc} = c_t(\zeta\dot{x}_t)$ as tire damper force.

By applying the Newton-Euler laws, the vehicle motion equations are as follows:

$$m_b\ddot{x}_b = -k_{f2}(\zeta_{bf2}) - c_{f2}(\dot{\zeta}_{bf2}) - k_{r2}(\zeta_{br2}) - c_{r2}(\dot{\zeta}_{br2}) - m_b g + u_f + u_r \quad (2)$$

$$j\ddot{\theta} = (k_{f2}(\zeta_{bf2}) + c_{f2}(\dot{\zeta}_{bf2}))(l_f\cos\theta) - (k_{r2}(\zeta_{br2}) + c_{r2}(\dot{\zeta}_{br2}))(l_r\cos\theta) \quad (3)$$

$$m_f\ddot{x}_f = k_{f2}(\zeta_{bf2}) + c_{f2}(\dot{\zeta}_{bf2}) - k_{f1}(\zeta_{bf1}) - c_{f1}(\dot{\zeta}_{bf1}) - m_f g + u_f \quad (4)$$

$$m_r\ddot{x}_r = k_{r2}(\zeta_{br2}) + c_{r2}(\dot{\zeta}_{br2}) - k_{r1}(\zeta_{br1}) - c_{r1}(\dot{\zeta}_{br1}) - m_r g + u_r \quad (5)$$

In above relations we have

$$\zeta_{bf2} = x_b - \zeta_{sf2} - x_f - l_f\sin\theta$$
$$\dot{\zeta}_{bf2} = \dot{x}_b - \dot{x}_f - \dot{\theta}l_f\cos\theta$$
$$\zeta_{br2} = x_b - \zeta_{sr2} - x_r + l_r\sin\theta$$
$$\dot{\zeta}_{br2} = \dot{x}_b - \dot{x}_r + \dot{\theta}l_r\cos\theta$$
$$\zeta_{bf1} = x_f - \zeta_{sf1} - x_{fd}$$
$$\dot{\zeta}_{bf1} = \dot{x}_f - \dot{x}_{fd}$$
$$\zeta_{br1} = x_r - \zeta_{sr1} - x_{rd}$$
$$\dot{\zeta}_{br1} = \dot{x}_r - \dot{x}_{rd} \quad (6)$$

where ζ_{sf2} and ζ_{sr2} are the static length variations of the suspension springs, ζ_{sf1}, ζ_{sr1} are the static length variations of the equal stiffness in tires. The simulation parameters numerical values are shown in Table 1.

3. Forcing frequency analysis

Dynamic simulation of the open loop system of the vehicle vertical motion under the active suspension system was performed by numerically solving the differential equations of the motion of the system based on the relations (2)-(5) with fourth order Runge-Kutta numerical method. The numerical values of the system parameters in the simulation system are considered according to table 1 and the values of the input excitation parameters of the road surface are as A=0.08m and phase α=π/9 rad. The system's responses in the steady state mode indicate the occurrence of chaos in the uncontrolled system, which the forcing frequency diagrams is used to prove the chaotic vibrations.

Table 1: Values of parameters in the numerical solutions

System parameters	Value
M_b	1180 kg
J	633.6 kg m^2
M_f	50 kg
M_r	45 kg
K_{f2}	36952 N/m
K_{r2}	30130 N/m
K_{f1}, K_{r1}	140000 N/m
C_{f2}	500 kg/s
C_{r2}	360kg/s
C_{f1},C_{r1}	10kg/s
l_f	1.123 m
l_r	1.377 m

The natural frequencies of the system are calculated from the relationship $[K]-\omega_n^2[M]=0$ and $[A]=[M]^{-1}[K]$ that are equal to the eigenvalues of the matrix [A]. These frequencies for the half-vehicle model after calculation in Matlab software are equal to

$$f_{n1}=1.0750\,\text{Hz},\quad f_{n2}=1.8234\,\text{Hz}$$
$$f_{n3}=9.4976\,\text{Hz},\quad f_{n4}=9.8139\,\text{Hz}$$

as can be seen from the graphs in figure (2), approximately at the frequency f=1.823Hz which is the dominant frequency of the system, the frequency of the system's excitation force is in the same range as the natural frequency of the system, and probability there is a phenomenon of frequency amplification. In order to verify the values of the natural frequencies, Table 2 summarizes the results obtained in this research compared to the results of reference [10]. The results of the comparisons showed that the natural frequencies obtained in this research are in the same range as the reference that clearly indicated the correctness of the calculations.

Table 2: Comparison of the results of natural frequencies are obtained in this research with reference [10]

	f_{n1}	f_{n2}	f_{n3}	f_{n4}
Natural frequency in this research (Hz)	1.0750	1.8234	9.4976	9.8139
Natural frequency in ref [10] (Hz)	1.28	1.80	9.08	9.26

The relationship between the speed of the vehicle and the frequency of the driving force is $f=v/\lambda$ where f is the frequency of the driving force and λ is the wavelength of the roughness of the road surface, which was previously defined as a sine wave. The values of the vehicle speed, taking into account the reference [6] and the values of the first and second natural frequency and the jump frequency [f=1.075, 1.8234, 3.6] Hz are equal to [v=12.92, 21.92, 43.28] km/h. The dynamic analysis of the frequency control parameter of the road surface excitation force is shown in the graphs of Figure (2), which includes the maximum absolute value of the displacement of the state variables according to the frequency control parameter of the road surface excitation force, which indicates different behaviors in the responses of the system with increasing and decreasing frequency of the driving force. The range of increasing and decreasing frequency, for example, in the frequency range 1Hz<f<6Hz in parts of the frequency range 3Hz<f<5Hz, we see the behavior of frequency jumping.

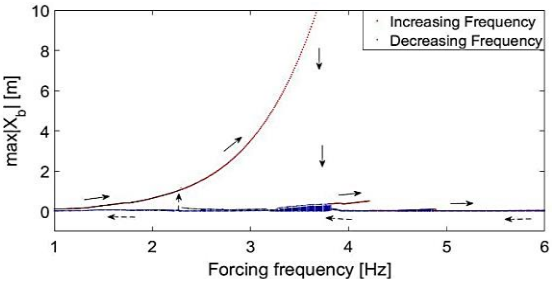

(a)

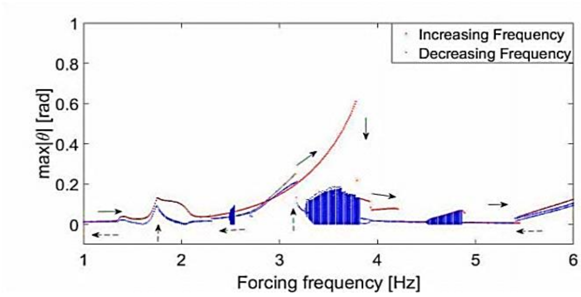

(b)

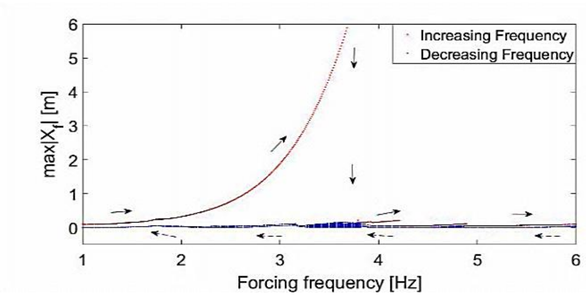

(c)

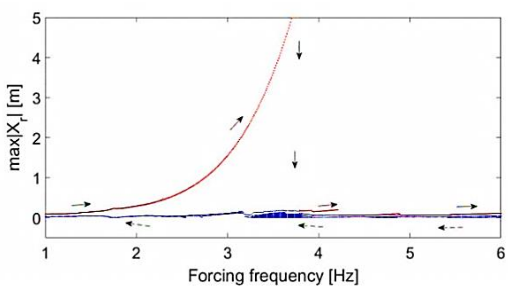

(d)

Figure 2: Frequency response diagrams for state variable when the forcing frequency f is slowly increased and decreased: (a) $\max|x_b(t)|$, (b) $\max|\theta(t)|$, (c) $\max|x_f(t)|$, and (d) $\max|x_r(t)|$

4. Chaos control system design

Sliding Chaos control via Pyragas method based on the delay feedback control for stabilizing the UPOs has been conducted, in which a UPO is estimated by a time-delay state variable. The feedback used in this control strategy is based on the difference between linear state and its time delay, and the time constant associated with the delay is considered to be equal to the periodic orbit of UPOs. One of the advantages of delay feedback is that it does not require basic knowledge of the UPOs except for its fluctuation period and can be easily implemented. Therefore, the control input signal is extracted in a simple way $u(t)=k[y(t-\tau)-y(t)]$ that is the output signal, τ is time delay and K is adjustable control gain, which by selecting appropriate value, ensures the stability of UPOs [2,3].

4.1. Delay feedback control algorithm

The Time delay feedback control algorithm is a linear feedback controller for stabilizing unstable periodic orbits in the system. If the dynamic system is defined as follows:

$$x^{(n)}=f(t,\underline{x})+g(t,\underline{x})u \tag{7}$$

where x is the state vector, u is the control input signal, f and g are uncertain functions and in u = 0, the system has chaotic behavior [17]. For this reason, at first, the delay state of is defined. It is obvious that the $\underline{\tilde{x}}(t)=\underline{x}(t-T)$ delay state should meet the following relation.

$$\tilde{x}^{(n)}=f(t-T,\underline{\tilde{x}})+g(t-T,\underline{\tilde{x}})\tilde{u} \tag{8}$$

where, $\tilde{u}=u(t-T)$. The dynamics of error system is obtained by distinguishing between two equations (7) and (8) as follows:

$$\begin{aligned}x^{(n)}-\tilde{x}^{(n)}&=f(t,\underline{x})-f(t-T,\underline{\tilde{x}})\\&+g(t,\underline{x})u-g(t-T,\underline{\tilde{x}})\tilde{u}\end{aligned} \tag{9}$$

where $\underline{e}=\underline{x}-\underline{\tilde{x}}$ the error vector and the differential equation of error system are expressed as follows:

$$\begin{aligned}e^{(n)}&=f(t,\underline{e}+\underline{\tilde{x}})-f(t-T,\underline{\tilde{x}})\\&+g(t,\underline{e}+\underline{\tilde{x}})u-g(t-T,\underline{\tilde{x}})\tilde{u}\end{aligned} \tag{10}$$

Therefore, the stability of an UPOs in a chaotic system according to equation (9) leads to the stabilization of the error dynamics (10) that in order to increase the speed of convergence of the system to its stable fixed points, due to the uncertainties of the system, the robust control strategy based on the sliding mode has been used with definition of the sliding surface as follows [17]:

$$S=\sum_{i=1}^{n+1}\alpha_i\hat{e}_i \tag{11}$$

where $\hat{e}_i(t)=\int_T^t e_i(s)ds=\int_T^t e^{(i-1)}(s)ds$ and $\alpha_i\rangle 0$ that to achieve a stable dynamic for reaching sliding mode, the system must be placed in $S=0$. In order to extract the control input u that satisfies the reaching mode and the trajectory of the system in a limited time to cross the intersection of the sliding surface, a definite positive Lyapunov exponent function is defined as $V=(1/2)S^2$, which is ultimately derived from the Lyapunov function and, assuming $g(t,\underline{x})\rangle 0$ and simplifying the calculations, the control input u is extracted as follows [17].

$$\begin{aligned}u=&-\frac{1}{\alpha_n g_m(t,\underline{x})}(\alpha_n\hat{f}(t,\underline{x})-\alpha_n\hat{f}(t-T,\underline{\tilde{x}})\\&+\sum_{i=1}^{n}\alpha_i e_i+K\text{sign}(S))\end{aligned} \tag{12}$$

where, the coefficient k in order to satisfy the Lyapunov stability condition of the system must apply to the following inequality.

$$\begin{aligned}K\geq&\left(\frac{g_M(t,\underline{x})}{g_m(t,\underline{x})}-1\right)\left|\sum_{i=1}^{n}\alpha_i e_i+\alpha_n f(t,\underline{x})-\alpha_n f(t-T,\underline{\tilde{x}})\right|\\&+\alpha_n F(t,\underline{x})+\alpha_n F(t-T,\underline{\tilde{x}})+g_M(t-T,\underline{\tilde{x}})|\tilde{u}|+\theta\end{aligned} \tag{13}$$

5. Stability and robustness analysis

The responses of closed loop system under the delay sliding mode controller that control gains are determined by the fuzzy logic depicts a stable behavior, since the responses of the simulated system are inclined towards their desired values in distinct time and are completely bounded. Also for the stability analysis of the feedback system, the Lyapunov stability criterion was used, which is based on the linearization of the system around the fixed point, the eigenvalues of the system are $\lambda_1=-0.56$, $\lambda_2=-7.87$, and $\lambda_{3,4}=-4.6\pm j0.343$ that placed in the left hand of the complex plane, which depicts system stability.

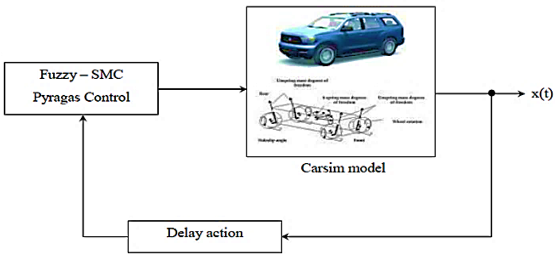

Figure 3: Feedback Control of block diagram in Carsim simulation

In order to consider the robustness of the designed controller, at first, the robustness of the control system against the parametric uncertainties is examined so that the mass and inertia moments of the vehicle model is increased as 8% of initial values and applied to the feedback system. Therefore, the new simulation results show the appropriate performance of the closed loop control system in compared with the changes of parameters. Also, in order to analyze the robustness of the controller relative to the structural and un-modeled uncertainties, the designed control system is linked to the Carsim software simulator and controller is applied to a SUV vehicle model with 27 degrees of freedom based on the figure 3. Ultimately, the results of feedback simulation in Carsim model indicates the entirely adaptation of controller responses in simulator with the designed feedback controller.

6. Control force of active suspension actuator

The force of the front and rear actuators of the active suspension system under the Time delay feedback controller is shown in figure (4) as below.

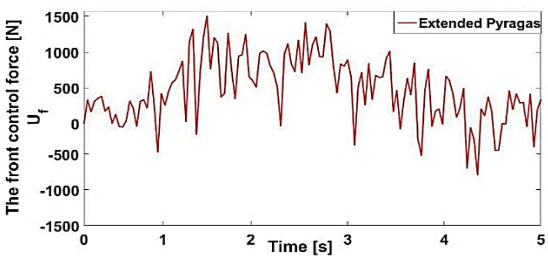

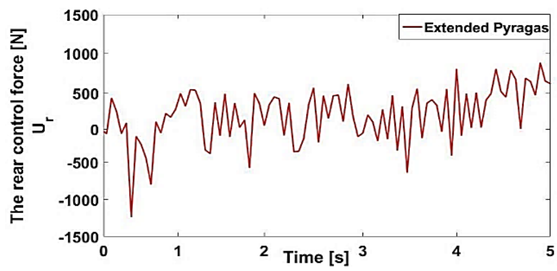

Figure 4: The front and rear actuator control force of active suspension

7. Power consumption

Actuator power consumption is very significant performance criteria in active suspension systems to quantify the proposed controllers. Power consumption P_{ac} can be determined using the following mathematical equation [18]:

$$P_{ac} = \frac{\int_0^T \left[U(t) \cdot (\dot{SWS})(t) \right] dt}{T} \qquad (14)$$

Where, U is the control force, SWS is the suspension working space across the actuator, and T is the simulation time. Figure (5) shows the displacements of the front and rear wheels relative to the vehicle body. According to figure (6), the average power consumption of the Time delay feedback controller for the front and rear suspension systems is equal to 1.2117kW and 0.4114kW, respectively. From the values of the average power consumption, it is evident that the average power consumption in the rear suspension system is lower than the front suspension system.

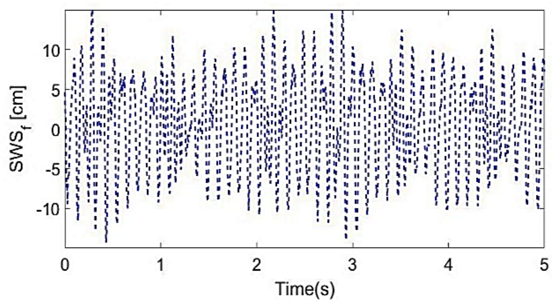

(a)

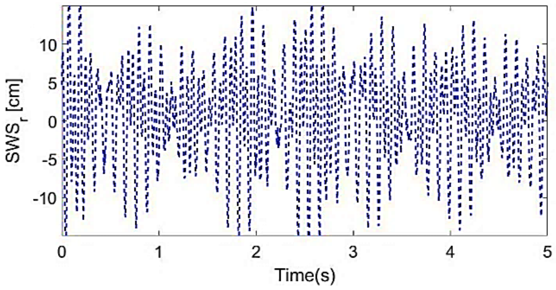

(b)

Figure 5: displacement of the front and rear wheels relative to the vehicle body, (a) displacement of the front wheel relative to the body, (b) displacement of the rear wheel relative to the body.

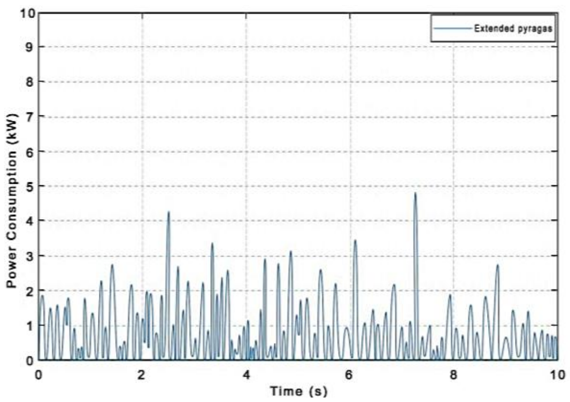

(a)

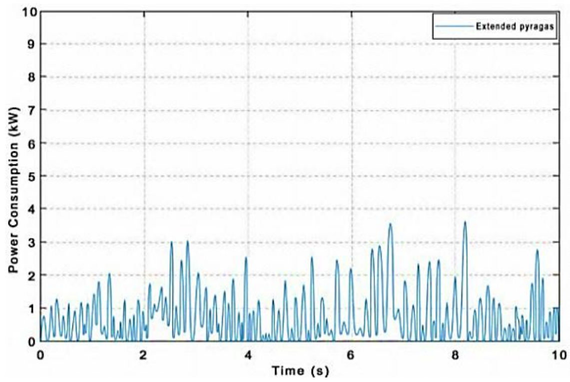

(b)

Figure 6: power consumption of the suspension system under the Time delay feedback controller, (a) front suspension system, (b) rear suspension system

8. Conclusion

The chaotic vibrations of the bounce model of vehicle in the face of uneven road surface were investigated in this paper, and then with the new sliding delay feedback fuzzy controller, the irregular oscillations are eliminated. Therefore, the mathematical model of the system is derived based on the Newton-Euler formulas and simulated the open loop system. Then forcing frequency diagrams are used to analyze the chaos in the nonlinear dynamics. According to the results of the forcing frequency diagram, the range of changes in control parameters in periodic, quasi-periodic, and chaotic behavior are demonstrated in the uncontrolled system that can be used in design of the control system in terms of disturbances and control signals values. In order to control the chaotic responses, chaos control based on the delay feedback strategy is developed with no need to solve the UPOs in the active suspension system. To increase the system rapid stabilization, a sliding mode control was used in the structure of time delay feedback controller. Also, in order to eliminate the chattering phenomenon in the sliding mode and to online estimate the controller gain accurately, the fuzzy inference system is combined with the sliding delay feedback system. The simulation results of the feedback system based on the Fuzzy SMC-Pyragas indicates the stabilization of the dynamics along with the elimination of chaotic behavior by reducing the settling time without any overshoot in the responses. Comparison of results in this work with [19] depicts 15% reduction at the settling time besides the system response overshoot rejection. Also the comparison of control signals the controller input amplitude with [19], in addition to 26% reduction in actuators effort, the saturation problems in suspension actuators can be solved and 34% decrease in the energy consumption according to the subplot area in the control signal diagram. Comparison with [20] depicts 20% reduction at the settling time by the system responses overshoots rejection. Also, compared to [20], in addition to 35% reduction in the amplitude of the controller input and delete the saturation problem in suspension actuators, 20% the energy consumption decrease was demonstrated in the control signal diagram. Additionally, the power consumption of the proposed controller was examined, whereas, the mean values of the power consumption in this work is improved as 48% relative to reference [18].

9. Notation

M_b	vehicle body mass
J	vehicle body inertia

M_f	front unsprung mass
M_r	rear unsprung mass
$X_b(t)$	displacement of M_b
$\theta(t)$	angular displacement of M_b
$X_f(t)$	displacement of M_f
$X_r(t)$	displacement of M_r
$X_{fd}(t)$	excitation to the front tire
$X_{rd}(t)$	excitation to the rear tire
l_f	front length
l_r	rear length
K_{f2}	front suspension spring stiffness
C_{f2}	front suspension damping coefficient
K_{r2}	rear suspension spring stiffness
C_{r2}	rear suspension damping coefficient
K_{f1}	front tire stiffness
C_{f1}	front tire damping coefficient
K_{r1}	rear tire stiffness
C_{r1}	rear tire damping coefficient
K_s	stiffness of the suspension springs
A	amplitude of the excitation force
f	frequency of the excitation force
u_f	the force of the front actuators of the active suspension system
u_r	the force of the rear actuators of the active suspension system
A	the time delay between the road roughness to the front and rear tires

References:

[1] E. Ott, C. Grebogi, JA. Yorke, Controlling chaos, Phys Rev Lett, (1990), 64:1196–1199.

[2] K. Pyragas, Continuous control of chaos by self-controlling feedback, Physics letters A, (1992), 170:421-428.

[3] K. Pyragas, A.Tamas, Experimental control of chaos by delayed self-controlling feedback, Phys. Lett. A, (1993), 180:99–102.

[4] M. Abtahi, Chaotic study and chaos control in a half-vehicle model with semi-active suspension using discrete optimal Ott–Grebogi–Yorke method, J Multi-body Dynamics, (2017), 231:148–155.

[5] G. Litak, M. Borowiec, M. Friswell, W. Przystupa, Chaotic response of quarter car model forced by a road profile with a stochastic component, Chaos, Solutions and Fractals, (2009), 39:2448–2456.

[6] Y. Chen, L. Chen, X. Xu, R. Wang, X. Yang, Chaotic Motion in a Nonlinear Car Model Excited by Multi-frequency Road Surface Profile, Chinese Journal of Mechanical Engineering, (2018), 30(1): 689–697

[7] R. Naik, P. Singru, Resonance, stability and chaotic vibration of a quarter car vehicle model with time-delay feedback, Common Nonlinear Sci Numer Simulat, (2011), 16:3397–3410.

[8] F. Pashaei, S. M. Abtahi, Chaotic Analysis and Chaos Control of a Lateral Dynamics Vehicle Based on the Nonlinear Poincaré Map with Fuzzy Controller, Automotive Science and Engineering, (2021), 11(4): 3693-3700.

[9] S.M. Abtahi, Melnikov-based analysis for chaotic dynamics of spin-orbit motion of a gyrostat satellite, Journal of Multi-body Dynamics, (2019), 233(4): 931-941.

[10] J. Fakheari, H. Khanlo, M. Ghayour, K. Faramarzi, The influence of road bumps characteristics on the chaotic vibration of a nonlinear full-vehicle model with driver, International Journal of Bifurcation and Chaos, (2016), 26:151-161.

[11] R. Dehghani, H. Khanlo, J. Fakhraei, Active chaos control of a heavy articulated vehicle equipped with Magnetorheological damper, Nonlinear Dyn, (2017), 87:1923–1942.

[12] Y. Kucukefe, K. Adnan, Delayed feedback control as applied to active suspension of a ground vehicle, Eurocon (2009), IEEE.

[13] Z. Zhang, K. Chau, Z. Wang, Analysis and Stabilization of Chaos in the Electric-Vehicle Steering System, IEEE Transactions on Vehicle Technology, (2013), 62:1-10.

[14] G. Koumen, M. Taffo, S. Siewe, C. Tchawoua, Stability switches and bifurcation in a two-degrees-of-freedom nonlinear quarter-car with small time-delayed feedback control, Chaos, Solitons and Fractals, (2016), 87: 226–239.

[15] M. Abtahi, Melnikov-based analysis for chaotic dynamics of spin-orbit motion of a gyrostat satellite, Journal of Multi-Body Dynamics, (2019), 233: 931-941.

[16] W. Chen, R. Zhang, L. Zhao, H. Wang, Zh. Wei, Control of chaos in vehicle lateral motion using the sliding mode variable structure control, Proc IMeche Part D:J Automobile Engineering, (2018), 1–14.

[17] H. Salarieh, A. Alasty, Chaos control in uncertain dynamical systems using nonlinear delayed feedback, Chaos, Solutions& Fractals, (2009), 41:67-71.

[18] Hassan. Metered, Ibrahim Musaad. Ibrahim, Vibration Mitigation of Commercial vehicle Active Tandem Axle suspension system, SAE internatiol journal Vol 18, (2022), 02-15-03-0015

[19] M. Abtahi, Suppression of chaotic vibrations in suspension system of vehicle dynamics using chattering-free optimal sliding mode control, Journal of the Brazilian Society of Mechanical Sciences and Engineering, (2019), 41:209-219.

[20] Y. N. Golouje, S. M. Abtahi, Chaotic dynamics of the vertical model in vehicles and chaos control of active suspension system via the fuzzy fast terminal slidin mode control. Journal of Mechanical Science and Technology, (2021), 35 (1) 31-43.